Unified approach to split absorbing boundary conditions for nonlinear Schrödinger equations: Two-dimensional case

Jiwei Zhang,[1,*] Zhenli Xu,[2,†] and Xiaonan Wu[1,‡]
[1]*Department of Mathematics, Hong Kong Baptist University, Kowloon, Hong Kong, People's Republic of China*
[2]*Department of Mathematics and Statistics, University of North Carolina at Charlotte, Charlotte, North Carolina 28223, USA*
(Received 7 January 2009; published 21 April 2009)

This paper aims to design local absorbing boundary conditions (LABCs) for the two-dimensional nonlinear Schrödinger equations on a rectangle by extending the unified approach. Based on the time-splitting idea, the main process of the unified approach is to approximate the kinetic energy part by a one-way equation, unite it with the potential energy equation, and then obtain the well-posed and accurate LABCs on the artificial boundaries. In the corners, we use the (1,1)-Padé approximation to the kinetic term and also unite it with the nonlinear term to give some local corner boundary conditions. Numerical tests are given to verify the stable and tractable advantages of the method.

DOI: 10.1103/PhysRevE.79.046711 PACS number(s): 02.70.Bf, 03.75.Lm, 42.25.Gy

I. INTRODUCTION

Many physical phenomena are modeled by Schrödinger-type equations on an unbounded domain such as gravity waves on deep water in fluid dynamics, pulse propagations in optics fibers, and Bose-Einstein condensation. How to numerically and efficiently solve these problems remains a challenge due to the principle difficulties of not only the unboundedness but also nonlinearities and high spatial dimensions. The common practice to overcome the unboundedness is to limit the domain of interest by an artificial boundary Γ, impose well-posed and accurate absorbing boundary conditions (ABCs), then solve the reduced approximate problems defined on the bounded domain. The procedure is usually called artificial boundary method, in which the design of suitable ABCs plays a core role. In the last decades, mathematicians, engineers, and physicists have been attracted and devoted to the study of this field, such as [1–5] and reviews [6–9]. In general, the artificial boundary conditions can be grouped into two categories, nonlocal and local ABCs. Global ABCs usually lead to the well-approximated and well-posed truncated problems; however, they are usually expensive for practical simulations. While local ABCs are computationally efficient and tractable, the accuracy and stability are the main concerns. Hence, an appropriate boundary condition implies two essential requirements:

(1) They are "easy" to discretize and "cheap" to compute in terms of the computational time;

(2) They combined with the governing equation on the computational domain result in well-posed problems.

Another approach worth to mention is the perfectly matched layer method [10], which has been applied to many complicated wave propagation problems.

In this paper, we consider the construction of high-accurate local absorbing boundary conditions (LABCs) for the nonlinear Schrödinger (NLS) equations

$$i\partial_t\psi = -\Delta\psi + V(x)\psi + f(|\psi|^2)\psi, \quad x \in \mathbb{R}^d, \quad t > 0, \tag{1}$$

$$\psi(x,0) = \psi^0(x), \quad x \in \mathbb{R}^d, \tag{2}$$

where $d=1$ or 2, $V(x)$ is the potential function, and $\psi^0(x)$ is the initial data with a compact support in a finite domain $\Omega_i \subset \mathbb{R}^d$. The nonlinear term $f(|\psi|^2)$ can be endowed with different forms to stand for different applications [11–13]. For example, $f(|\psi|^2)=g|\psi|^2$ corresponds to a defocusing ($g>0$) or a focusing ($g<0$) effect of the cubic nonlinearity, which appears in the nonlinear optic for laser beam propagation [14–16]. Other nonlinearities such as the quintic nonlinearity [17] are also widely considered. For the linear Schrödinger equation, ABCs or the so-called transparent boundary conditions have been widely discussed in the early literatures [18–23] and references therein.

The second essential difficulty of the numerical solution for problem (1) is the nonlinearity. Generally, it is difficult for nonlinear problems to design some efficient ABCs. Several strategies have been developed such as the linearized or reduced method [24–27], operator splitting method [28–31], and references therein. For the nonlinear Schrödinger equation, although the things turn to be much more complicated, there has been still some new progress [32–40] recently, mostly focusing on the cubic nonlinearity. This paper extends the unified approach [41] to obtain efficient LABCs for the NLS equations on a rectangle boundary. For the multidimensional case, the corners always bring us in lots of trouble. By performing the (1,1)-Padé expansion to the energy operator and uniting it with the nonlinear term, we achieve the corresponding absorbing boundary conditions at corners. The obtained nonlinear LABCs are "easy" to discretize and can efficiently absorb the "fast" or "low" waves by adjusting the wave-number parameter involved in the LABCs. Furthermore, we investigate the well-posedness of the reduced problems defined on the computational domain with the obtained LABCs by a normal mode analysis. Some numerical examples are given to verify the attractive advantages of the method.

The organization of this paper is as follows. In Secs. II and III, we give a detailed description of our unified ap-

*jwzhang@math.hkbu.edu.hk
†xuzl@ustc.edu
‡xwu@hkbu.edu.hk

proach for designing the local absorbing boundary conditions. Section IV considers the stability of the reduced initial boundary problem on the truncated domain and the adaptive selection of the parameter wave number. We end the paper by giving some numerical examples to prove the effective and tractable advantages of our obtained LABCs.

II. UNIFIED APPROACH FOR ONE-DIMENSIONAL MODEL

To understand the spirit of the unified approach to local absorbing boundary conditions, let us briefly give an overview of its basic idea from the one-dimensional case [41]. Rewrite Eq. (1) in operator form on the artificial boundaries Γ as follows:

$$i\partial_t\psi(x,t) = (\hat{T} + \hat{V})\psi(x,t), \tag{3}$$

where operators $\hat{T}$ and $\hat{V}$ read

$$\hat{T} = -\partial_x^2 \text{ and } \hat{V} = V(x) + f(|\psi|^2). \tag{4}$$

The well-known time-splitting method (or the split-step method) implies that the wave propagation carries out the action of a kinetic energy step and a potential energy step separately for small time size τ. By Baker-Campbell-Hausdorff theorem, in a time interval from t to $t+\tau$ for τ small enough, the exact solution of Eq. (3) can be approximated by

$$\psi(x,t+\tau) \approx e^{-i\hat{T}\tau}e^{-i\hat{V}\tau}\psi(x,t). \tag{5}$$

which has the first order error $O(\tau)$ arising from the noncommutativity of the operators $\hat{T}$ and $\hat{V}$ [42]. For the second-order error $O(\tau^2)$, the Strang splitting [28] is widely used by

$$\psi(x,t+\tau) \approx e^{-i\hat{T}\tau/2}e^{-i\hat{V}\tau}e^{-i\hat{T}\tau/2}\psi(x,t). \tag{6}$$

The approximations in Eqs. (5) and (6) correspond to two subproblems: the linear subproblem and nonlinear subproblem. By adding some LABCs for linear subproblem, and solving the nonlinear subproblem (ODE) directly at the same time step, Refs. [33,43] show that this method is effective to numerically solve nonlinear Schrödinger-type equations. This approach is basically a two-step method. The difficulty is due to the nonlinearity of the problem, they only obtained the LABCs for linear subproblem. Can we obtain a LABC which can be applied to the nonlinear problems directly? Toward this goal, we use the operator form

$$\psi(x,t+\tau) = e^{-i[\hat{T}+\hat{V}]\tau}\psi(x,t), \tag{7}$$

which captures the information of the kinetic and nonlinear energy together. A clear advantage of the direct method is that the method is tractable. Another advantage of the direct method is that the method is showed stable, while the stability of the two step method is unknown. By differing from the left-going waves and right-going waves, from paper [41] the kinetic operator $\hat{T}$ can be approximated by

$$\hat{T} \approx \hat{T}^{(2)} = -\left(\pm i2k_0\frac{\partial}{\partial x} + k_0^2\right), \tag{8}$$

$$\hat{T} \approx \hat{T}^{(3)} = -(i\partial_x \pm 3k_0)^{-1}(3ik_0^2\partial_x \pm k_0^3), \tag{9}$$

which correspond to the second- and third-order local boundary conditions, respectively. The wave-number parameter $k_0=\sqrt{\omega_0}$ is used to adjust the efficiency of the boundary conditions and the frequency ω_0 is a positive constant. Substituting $\hat{T}^{(n)}$ for $\hat{T}$ in the first approximation in Eq. (7) yields the one-way approximate equations

$$i\partial_t\psi(x,t) = [\hat{T}^{(n)} + \hat{V}]\psi(x,t). \tag{10}$$

By a simple calculation, the nonlinear absorbing boundary conditions of order 2 and 3 are given by

$$n=2: \quad i\partial_t\psi \pm i2k_0\partial_x\psi = [-k_0^2 + V(x) + f(|\psi|^2)]\psi, \tag{11}$$

$$n=3: \quad i(i\partial_x \pm 3k_0)\partial_t\psi = [-(3ik_0^2\partial_x \pm k_0^3) + \{V(x) + f(|\psi|^2)\} \times (i\partial_x \pm 3k_0)]\psi. \tag{12}$$

Thus we obtain the local absorbing boundary conditions for nonlinear Schrödinger-type equations on the artificial boundaries.

III. UNIFIED APPROACH FOR MULTIDIMENSIONAL MODEL

A. Multidimensional linear equations

The above adopted strategy for constructing the nonlinear LABCs issued from the linear model, i.e., was to obtain the approximation of the kinetic term. Now we recall the linear equation in two dimensions

$$i\partial_t\psi = -(\partial_x^2 + \partial_y^2)\psi, \quad (x,y) \in \mathbb{R}^2. \tag{13}$$

In frequency domain, Eq. (13) implies the dispersion relation

$$\xi^2 + \eta^2 = \omega, \tag{14}$$

where ξ is the wave number in the x direction and η is the wave number in the y direction. Let the computational domain $\Omega_i=]0,L[^2$. The following plus sign in "$\pm$" corresponds to the positive direction, the minus sign to the negative direction, respectively. On the east and west artificial boundaries $\Gamma_e=\{(x,y)|x=L, 0<y<L\}$, $\Gamma_w=\{(x,y)|x=0, 0<y<L\}$, we have the corresponding dispersion relation of Eq. (14),

$$\xi = \pm\sqrt{\omega - \eta^2}. \tag{15}$$

By using the (1,1)-Padé approximation [21] for the square root in the dispersion relation (15), we obtain

$$\xi = \pm\sqrt{\omega - \eta^2} \approx \pm\xi_0\frac{1+3z}{3+z}, \tag{16}$$

where $z=\frac{\omega-\eta^2}{\xi_0^2}$ and ξ_0 is a wave-number parameter to adjust the efficiency of the approximation in the x direction. Simplifying Eq. (16) and solving the result, we have

$$\omega = \frac{\pm\xi_0^3 - 3\xi_0^2\xi - (\pm 3\xi_0\eta^2) + \xi\eta^2}{\xi \pm 3\xi_0}. \tag{17}$$

By the same argument as Eq. (16), we can obtain the approximate dispersive equation for frequency vector (ξ,η) on the northern and southern boundaries $\Gamma_n=\{(x,y)|y=L,0<x<L\}$, $\Gamma_s=\{(x,y)|y=0,0<x<L\}$,

$$\omega=\frac{\pm\eta_0^3-3\eta_0^2\eta-(\pm 3\eta_0\xi^2)+\eta\xi^2}{\eta\pm 3\eta_0}. \tag{18}$$

In fact, identity (18) follows directly Eq. (17) by exchanging ξ with η, and η_0 is the expand point in the y direction. Now we focus on the algebraic relations on four corners. By utilizing formula (9), one can see that the kinetic operator $\hat{T}$ can be approximated by using the (1,1)-Padé expansion. Applying the expansion to both ξ^2 and η^2 with the corresponding expansion point (ξ_0,η_0), we have

$$\omega=-\xi_0^2\frac{-3\xi\pm\xi_0}{-\xi\pm 3\xi_0}-\eta_0^2\frac{-3\eta\pm\eta_0}{-\eta\pm 3\eta_0}. \tag{19}$$

In identity (19), the plus sign in "±" is used at the northeast corner (L,L), the minus at the southwest corner (0,0). The approximations at the northwest corner $(0,L)$ and the southeast corner $(L,0)$ read, respectively,

$$\omega=-\xi_0^2\frac{3\xi+\xi_0}{\xi+3\xi_0}-\eta_0^2\frac{-3\eta+\eta_0}{-\eta+3\eta_0}, \tag{20}$$

$$\omega=-\xi_0^2\frac{-3\xi+\xi_0}{-\xi+3\xi_0}-\eta_0^2\frac{3\eta+\eta_0}{\eta+3\eta_0}. \tag{21}$$

By performing the inverse transformation into the physical space, one can obtain the local absorbing boundary conditions for linear equation [21,43]. Section III B will discuss how to obtain some efficient ABCs for the nonlinear equations.

B. Unified approach for multidimensional NLS equations

We have obtained the approximate dispersion relation for the linear equation in two dimensions, which can yield its LABCs after applying the dual correspondences $\xi\leftrightarrow -i\partial_x$, $\eta\leftrightarrow -i\partial_y$, and $\omega\leftrightarrow i\partial_t$ between frequency and physical domains. By straightforwardly extending the technique of 1D NLS equation, we similarly use the operator form of Eq. (1),

$$i\partial_t\psi(x,y,t)=[\hat{T}+\hat{V}]\psi(x,y,t), \tag{22}$$

where $\hat{T}$ stands for the linear differential operator, and $\hat{V}$ for the nonlinear operator, provided by

$$\hat{T}=-\partial_x^2-\partial_y^2 \quad \text{and} \quad \hat{V}=f(|\psi|^2)+V(x,y). \tag{23}$$

It is obvious to see that the kinetic operator $\hat{T}$ can be approximated by the corresponding differential operator $\hat{T}^{(3)}$ from the algebraic Eq. (17), Eq. (18), or Eq. (19), which are the third-order local boundary conditions at the artificial boundaries and the corners. Taking Eq. (17) as an example and using the dualities, on the east and west boundaries we have the approximate operators

$$\hat{T}^{(3)}=\frac{\pm\xi_0^3+3i\xi_0^2\partial_x\pm 3\xi_0\partial_y^2-\partial_x\partial_y^2}{-i\partial_x\pm 3\xi_0}.$$

Substituting $\hat{T}^{(3)}$ into Eq. (22), we have the approximate equations

$$i\partial_t\psi(x,y,t)=[\hat{T}^{(3)}+\hat{V}]\psi(x,y,t), \tag{24}$$

which also can be rewritten as

$$\begin{aligned}(\partial_x\pm 3i\xi_0)\partial_t\psi(x,y,t)&=[(\pm\xi_0^3+3i\xi_0^2\partial_x\pm 3\xi_0\partial_y^2-\partial_x\partial_y^2)\\&\quad+\hat{V}(-i\partial_x\pm 3\xi_0)]\psi(x,y,t).\end{aligned} \tag{25}$$

By simplifying Eq. (25), we obtain the nonlinear LABCs on the east and west boundaries as follows:

$$\begin{aligned}&-i(3\xi_0^2-V)\partial_x\psi+\partial_x\partial_t\psi-i\partial_x\partial_y^2\psi\\&\quad=\pm\xi_0(\xi_0^2-3V)\psi\pm 3i\xi_0\partial_t\psi\pm 3\xi_0\partial_y^2\psi\\&\quad\quad-f(|\psi|^2)(i\partial_x\psi\pm 3\xi_0\psi).\end{aligned} \tag{26}$$

By the same argument, we can achieve the corresponding LABCs on the other boundaries as follows:

$$\begin{aligned}&-i(3\eta_0^2-V)\partial_y\psi+\partial_y\partial_t\psi-i\partial_y\partial_x^2\psi\\&\quad=\pm\eta_0(\eta_0^2-3V)\psi\pm 3i\eta_0\partial_t\psi\pm 3\eta_0\partial_x^2\psi\\&\quad\quad-f(|\psi|^2)(i\partial_y\psi\pm 3\eta_0\psi).\end{aligned} \tag{27}$$

Also we can obtain the boundary conditions at corners: BC at the northeast corner (L,L),

$$\begin{aligned}&3\xi_0\partial_y\partial_t\psi+3\eta_0\partial_x\partial_t\psi+[3\xi_0^2+3\eta_0^2-V-f(|\psi|^2)]\partial_x\partial_y\psi\\&\quad-i\xi_0[\xi_0^2+9\eta_0^2-3V-3f(|\psi|^2)]\partial_y\psi+i\partial_x\partial_y\partial_t\psi\\&\quad-9i\xi_0\eta_0\partial_t\psi-i\eta_0[\eta_0^2+9\xi_0^2-3V-3f(|\psi|^2)]\partial_x\psi\\&\quad+3\xi_0\eta_0[3V+3f(|\psi|^2)-\xi_0^2-\eta_0^2]\psi=0,\end{aligned} \tag{28}$$

BC at the southwest corner (0,0),

$$\begin{aligned}&-3\xi_0\partial_y\partial_t\psi-3\eta_0\partial_x\partial_t\psi+[3\xi_0^2+3\eta_0^2-V-f(|\psi|^2)]\partial_x\partial_y\psi\\&\quad+i\xi_0[\xi_0^2+9\eta_0^2-3V-3f(|\psi|^2)]\partial_y\psi+i\partial_x\partial_y\partial_t\psi\\&\quad-9i\xi_0\eta_0\partial_t\psi+i\eta_0[\eta_0^2+9\xi_0^2-3V-3f(|\psi|^2)]\partial_x\psi\\&\quad+3\xi_0\eta_0[3V+3f(|\psi|^2)-\xi_0^2-\eta_0^2]\psi=0,\end{aligned} \tag{29}$$

BC at the southeast corner $(L,0)$,

$$\begin{aligned}&-3\xi_0\partial_y\partial_t\psi+3\eta_0\partial_x\partial_t\psi-[3\xi_0^2+3\eta_0^2-V-f(|\psi|^2)]\partial_x\partial_y\psi\\&\quad+i\xi_0[\xi_0^2+9\eta_0^2-3V-3f(|\psi|^2)]\partial_y\psi-i\partial_x\partial_y\partial_t\psi\\&\quad-9i\xi_0\eta_0\partial_t\psi-i\eta_0[\eta_0^2+9\xi_0^2-3V-3f(|\psi|^2)]\partial_x\psi\\&\quad+3\xi_0\eta_0[3V+3f(|\psi|^2)-\xi_0^2-\eta_0^2]\psi=0,\end{aligned} \tag{30}$$

and BC at the northeast corner $(0,L)$,

$$3\xi_0\partial_y\partial_t\psi - 3\eta_0\partial_x\partial_t\psi - [3\xi_0^2 + 3\eta_0^2 - V - f(|\psi|^2)]\partial_x\partial_y\psi - i\xi_0[\xi_0^2 + 9\eta_0^2 - 3V - 3f(|\psi|^2)]\partial_y\psi - i\partial_x\partial_y\partial_t\psi - 9i\xi_0\eta_0\partial_t\psi + i\eta_0[\eta_0^2 + 9\xi_0^2 - 3V - 3f(|\psi|^2)]\partial_x\psi + 3\xi_0\eta_0[3V + 3f(|\psi|^2) - \xi_0^2 - \eta_0^2]\psi = 0. \quad (31)$$

Hence, we obtain the explicit LABCs for two-dimensional (2D) nonlinear equations on the rectangular artificial boundaries and corners.

IV. STABILITY ANALYSIS FOR HARMONIC SOLUTIONS

Here we consider the well-posedness of the problem in the computational domain Ω_i with the obtained LABCs. Concerning the model Eq. (1), in which the function $f(s)$ can be chosen as different forms in different physical problems, the problem is more complicated because of the nonlinearities. The usual energy methods seem to be difficult to obtain the energy bound even for the simple 1D problem with order $n=2$; one can refer to [18,32,35] and references therein. Therefore, we use the normal mode analysis method [20,44] to investigate the model problem when it admits a progressive plane-wave solution [45]

$$\psi(x,t) = A \cdot e^{st+\xi x+\eta y}. \quad (32)$$

For one-dimensional case, the authors in [41] examined the stability and conclude that, for $V+f=v_1+f_1+i(v_2+f_2)$, the induced initial boundary value problem is well posed if functions $V(\cdot)$ and $f(\cdot)$ satisfy $v_2+f_2\leq 0$ in a small enough time size. Numerical examples also verify their stabilities. Now we extend the method to two dimensions. We first recall the philosophy of the general algebraic normal mode analysis, which is issued from the fact that the well-posed problem admits the complex eigenvalues with negative real parts $\mathrm{Re}(s)<0$, or generalized eigenvalues with $\mathrm{Re}(s)=0$ and the positive (negative) group velocity of the normal mode on the right-hand (left-hand) boundary. If there exist such eigenvalues, the solution will decrease with normal mode e^{st} and is hence stable. If there exist such generalized eigenvalues, the boundary conditions will admit an outgoing wave which will propagate energy into the exterior domain not to disrupt the solution in the computational domain or generate a spurious wave solution. By the way, design of the LABCs is based on the assumption that the one-way equation only admits the outgoing waves. This is because the eigenvalues or generalized eigenvalues satisfy the dispersion relations of both the model equation and the equations on the artificial boundaries. To calculate the eigenvalues or generalized eigenvalues, we replace the two-dimensional plane-wave form into Eq. (22) and boundary conditions (26) and (27). Without loss of generality, we take the east boundary conditions as an example. By the same arguments, one can obtain the similar results on the other boundaries. The parameters $\xi=k\cos\phi$ and $\eta=k\sin\phi$ are the wave numbers in the x and y directions, respectively, where ϕ is the angle of the direction of k measured from the normal of the boundary. Substituting the plane wave into Eq. (22) and the east boundary condition yields

$$is = -\xi^2 - \eta^2 + V + f(|\psi|^2), \quad (33)$$

$$is = \frac{i\xi_0(\xi_0^2 + 3\xi_0\eta^2 - 3V) - \xi(3\xi_0^2 - V)}{\xi - 3\xi_0 i} + f(|\psi|^2). \quad (34)$$

Solving the algebraic Eqs. (33) and (34) leads to

$$(\xi - i\xi_0)^3 + 3i\xi_0\eta^2(\xi_0 - 1) = 0. \quad (35)$$

Noticing that $\eta=k\sin\phi=0$ on the boundary $x=L$, we obtain from Eq. (35),

$$\xi = i\xi_0 \text{ and } s = -i\xi_0^2 - i(v_1+f_1) + (v_2+f_2). \quad (36)$$

Obviously, one gets $\mathrm{Re}(s)\leq 0$ for $v_2+f_2\leq 0$ from Eq. (36). Since the boundary conditions are designed to minimize all the outgoing waves, this implies that the group velocity is positive on the right-hand boundary and negative on the left-hand boundary. Hence there exists no generalized eigenvalue which will propagate energy into the interior domain to disrupt the true wave solution. If any instabilities caused by the generalized eigenvalues of the ABCs happen, they would not propagate energy to disrupt the interior solution. Hence, we conclude that the obtained 2D LABCs with the governing equation in the computational domain are stable.

Choose the parameters adaptively

The best choice of parameter $k_0=\sqrt{w_0}$ related to the frequency of wave impinged on the artificial boundary, exactly speaking, is half of the group velocity of the waves. The main reason is that the Padé approximation corresponds to the expansion point w_0 and would be more accurate when w_0 is closer to the frequency w. The relation between group velocity C and wave number k is

$$C = \frac{\partial\omega}{\partial k} = 2k.$$

It is natural to ask how to select suitable parameters adaptively such that the ABCs can annihilate all the incident waves efficiently. It is known that the initial wave is composed of waves with different group velocities; they will reach the artificial boundary separately. The previous papers proposed two strategies; we recapitulate them as follows. A first strategy suggested by Fevens and Jiang [20] is to use the Fourier series expansion of the physical variable in space and to take the positive components such that its Fourier mode is dominant by obtaining the frequency information over the whole computational domain. Another strategy proposed by Xu *et al.* [43] is to utilize the Gabor transform in the vicinity of the artificial boundary. In the frequency domain the Gabor transform is given by

$$\hat{\psi}(k,t) = \int_{x_l}^{x_r} W(x)\psi(x,t)e^{-ikx} = \int_{x_l-b}^{x_r} \psi(x,t)e^{-ikx}, \quad (37)$$

where the window function is

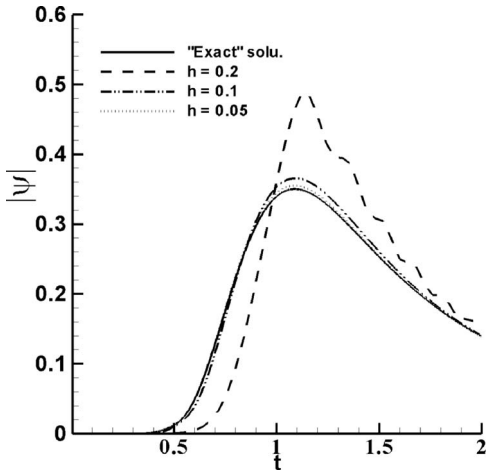

FIG. 1. Evolution of numerical solutions with different mesh sizes at corner (10,10).

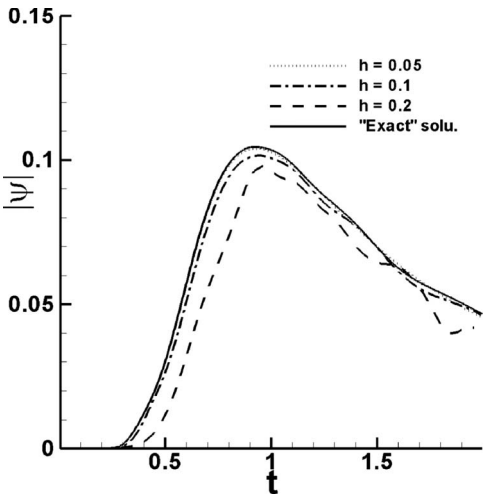

FIG. 2. Evolution of numerical solutions with different mesh sizes at point (10,5).

$$W(x) = \begin{cases} 1, & x \in [x_r - b, x_r], \\ 0, & \text{otherwise}, \end{cases}$$

with b denoting the window width. Two choices for k_0: the first one is to take the frequency such that its spectrum is the maximum, i.e.,

$$|\hat{\psi}(k_0,t)| = \sup_{k\geq 0}\{|\hat{\psi}(k,t)|\}, \tag{38}$$

the second choice is to utilize the energy-weighted wavenumber parameter selection approach as

$$k_0 = \frac{\int_0^\infty |\hat{\psi}(k,t)|^m k dk}{\int_0^\infty |\hat{\psi}(k,t)|^m dk}, \tag{39}$$

with m a positive real number. We remark that the second Eq. (39), improved the first Eq. (38), and they are equivalent to each other when $m=+\infty$. The authors in [43] suggest $m=4$ is a good choice based on numerical experiments.

V. NUMERICAL IMPLEMENTATION AND EXAMPLES

In the computational domain $]0,L[^2$, let Δx, Δy, and Δt be the grid sizes in spaces and time. Denote operators D_+, D_-, and D_0 by the forward, backward, and centered differences, respectively, and S_+, S_-, and S_0 by the forward, backward, and centered sums; for example,

$$D_+^x \psi_{\iota,j}^n = (\psi_{\iota+1,j}^n - \psi_{\iota,j}^n)/\Delta x, S_+^t \psi_{\iota,j}^n = (\psi_{\iota,j}^{n+1} + \psi_{\iota,j}^n)/2.$$

$\psi_{\iota,j}^n$ represents the approximation of the function ψ at the grid point (x_ι, y_j, t^n). We test the performance of the obtained LABCs by using the following linearized Crank-Nicolson scheme [40,45] for the discretization in interior domains

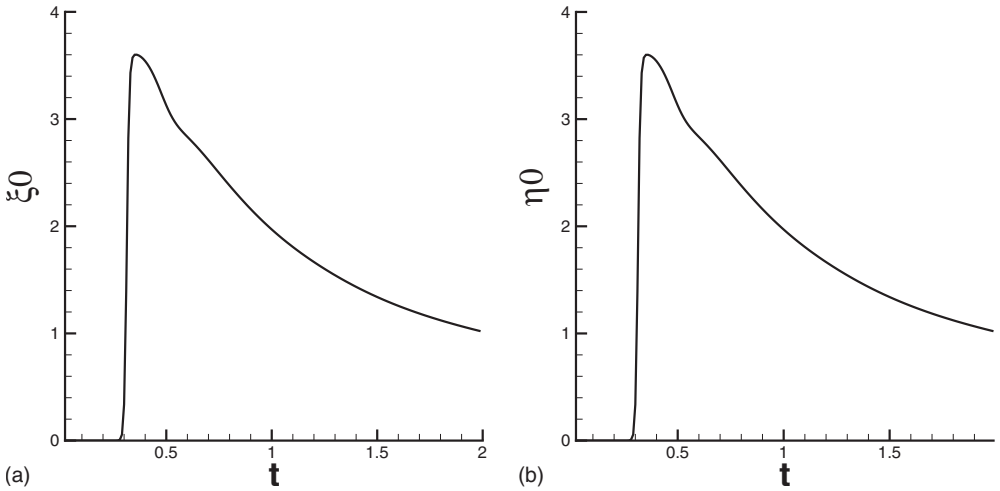

FIG. 3. Evolutions of parameters ξ_0, η_0 by using Gabor transform adaptively.

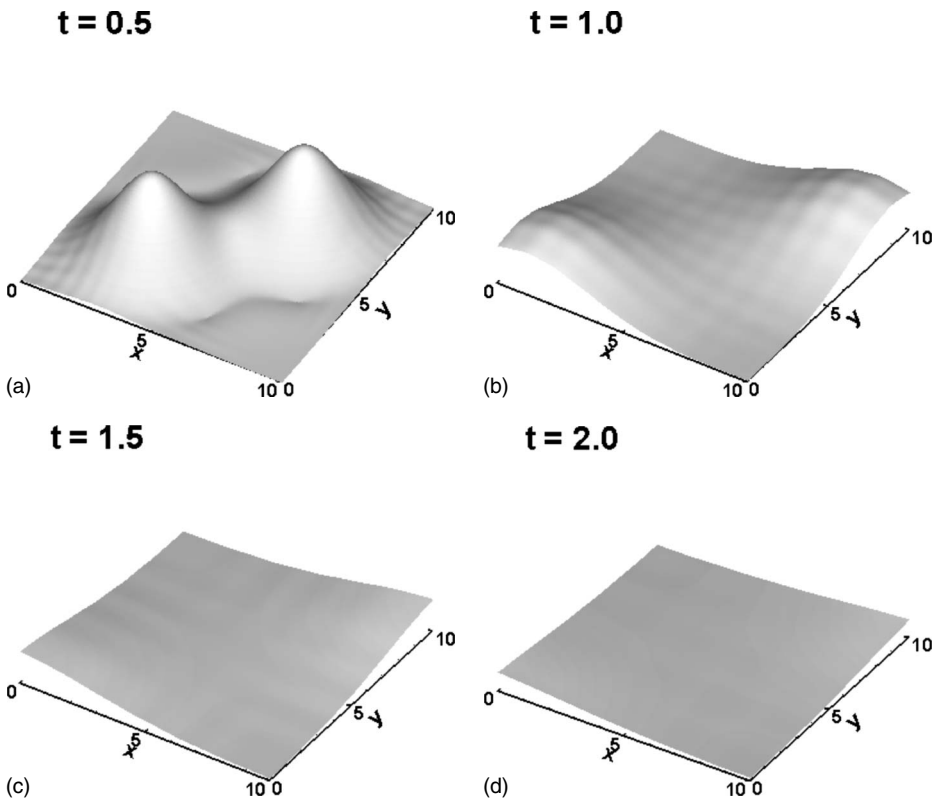

FIG. 4. The contour of the numerical solution at different time.

$$iD_+^t\psi_{ij}^n = -(D_+^xD_-^x + D_+^yD_-^y)S_+^t\psi_{ij}^n + \left[V_{ij} + \frac{3}{2}f(|\psi_{ij}^n|^2) - \frac{1}{2}f(|\psi_{ij}^{n-1}|^2)\right]S_+^t\psi_{ij}^n, \quad (40)$$

with the order of the truncated error $O(\Delta t^2+\Delta x^2+\Delta y^2)$, where the nonlinear term is approximated by the known variables through an extrapolation technique so that nonlinear iteration can be avoided. Now we focus on the approximation on the artificial boundary and take the east boundary condition (26) as example; the discretized forms are given by

$$\psi_x = D_-^xS_+^t\psi_{I,j}^n, \quad \psi = S_-^xS_+^t\psi_{I,j}^n, \quad \psi_{yy} = S_-^xD_-^yD_+^yS_+^t\psi_{I,j}^n, \quad (41)$$

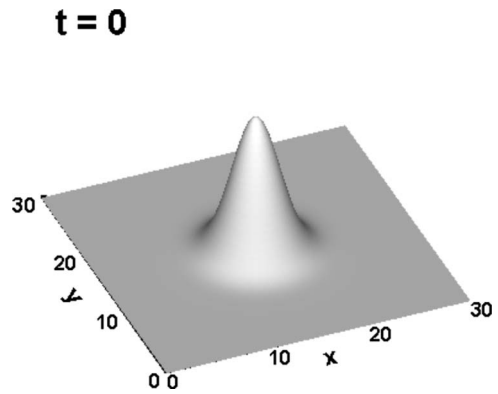

FIG. 5. The initial Gaussian pulse.

$$\psi_t = S_-^xD_+^t\psi_{I,j}^n, \quad \psi_{xyy} = D_-^xD_+^yD_-^yS_+^t\psi_{I,j}^n, \quad \psi_{xt} = D_-^xD_+^t\psi_{I,j}^n, \quad (42)$$

and the discretized forms in the corner boundary condition (28) are given by

$$\psi_x = D_-^xS_-^yS_+^t\psi_{I,J}^n, \quad \psi = S_-^xS_-^yS_+^t\psi_{I,J}^n, \quad \psi_y = S_-^xD_+^yS_+^t\psi_{I,j}^n, \quad (43)$$

$$\psi_t = S_-^xS_-^yD_+^t\psi_{I,J}^n, \quad \psi_{xy} = D_-^xD_-^yS_+^t\psi_{I,J}^n, \quad \psi_{xt} = D_-^xS_-^yD_+^t\psi_{I,J}^n, \quad (44)$$

$$\psi_{xyt} = D_-^xD_-^yD_+^t\psi_{I,J}^n, \quad \psi_{yt} = D_-^yS_-^xD_+^t\psi_{I,J}^n, \quad (45)$$

and $f(|\psi_{I,j}|^2)=\frac{3}{2}f(|\psi_{I,j}^n|^2)-\frac{1}{2}f(|\psi_{I,j}^{n-1}|^2)$. By the same way, the discretizations can be achieved for the other three boundaries and three corners. Thus the full-discrete scheme is obtained for the two-dimensional nonlinear case, which is a linear algebraic system at each time step.

Example 1. In this example, for the two-dimensional NLS Eq. (1) by using the linearized Crank-Nicolson scheme, we take the nonlinearity $f(|\psi|^2)=-|\psi|^2$, the potential $V\equiv 0$, and the initial function

$$\psi(x,y,0) = \sqrt{2}e^{-(x-x_0)^2-(y-y_0)^2}e^{2i(x+y-x_0-y0)^2}$$

with the centered point $(x_0,y_0)=(5,5)$. This test can be seen in [43]. The wave will propagate into the northwest corner and arrive to the corner around $t=0.4$ when L is chosen by

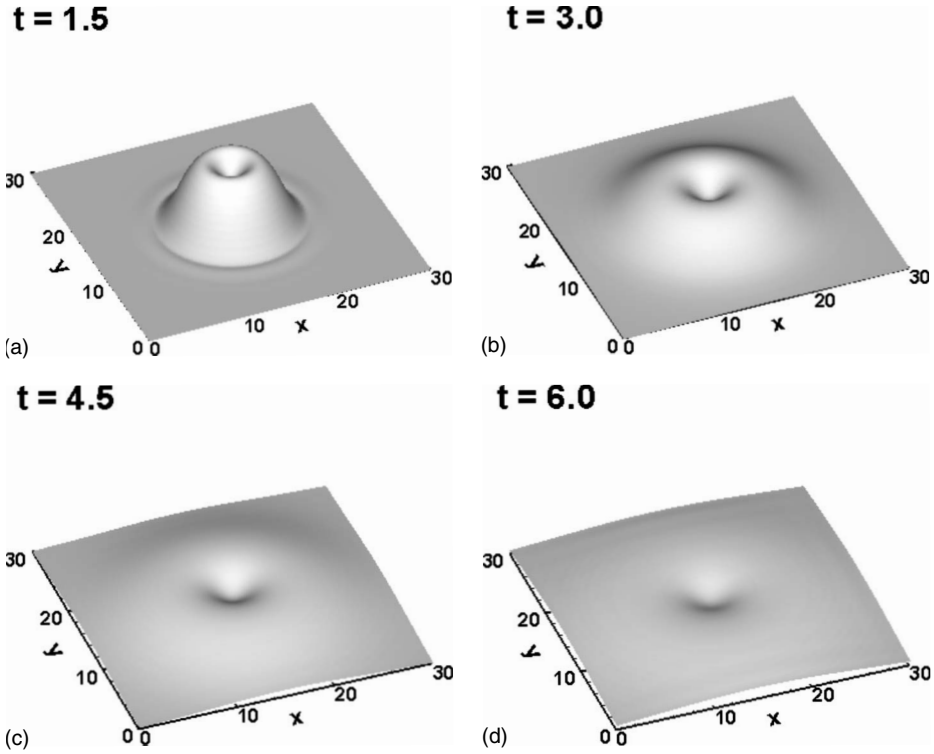

FIG. 6. The contour of the numerical solution at different time.

10. In the computational domain $]0,10[^2$, Figs. 1 and 2 plot the evolutions of the numerical solutions with different mesh sizes ($h=\Delta x=\Delta y$) at two points (10,10) and (10,5), respectively. The reference "exact" solution is obtained by computing a larger box $]0,20[^2$ with mesh size $\Delta x=\Delta y=0.05$ and $\Delta t=\Delta x^2$. To choose the parameters ξ_0, η_0 adaptively, we set the window length of the Gabor transform $b=L/4$ and $m=4$ along x and y directions, respectively. The evolutions of ξ_0, η_0 are shown in Fig. 3. One can see that the values at the corner tend to the "exact" solution quickly when small meshes are used. To further investigate the efficiency of the LABCs at corners, we set the initial value of the wave

$$\psi(x,y,0) = \sqrt{2}e^{-(x-x_0)^2-(y-y_0)^2}e^{2i(x+y-x_0-y0)^2} + \sqrt{2}e^{-(x-x_0)^2-(y-y_0)^2}e^{-2i(x+y-x_0-y0)^2},$$

with the centered point $x_0=5$ and $y_0=5$. This wave packet moves along the northeast and southwest directions, and will impinge on the artificial boundaries Γ_e, Γ_n Γ_s, Γ_w and northeast and southwest corners, respectively. Figure 4 shows the contours of the numerical solution $|\psi|$ at time $t=0.5$, 1, 1.5, and 2 under mesh size $\Delta x=\Delta y=0.05, \Delta t=\Delta x^2$ in the domain $]0,L[^2$ with $L=10$. Few reflections can be observed. Observe that if we set the parameters ξ_0, η_0 as a fixed value about 2.0, we can also obtain the same desired numerical solutions. In fact, the parameter can be chosen in a larger interval. For soliton solutions of the NLS equation, the adaptive choice of parameter is efficient based on the numerical experiments [43].

Example 2. In the second example, the nonlinear term is chosen as $f(|\psi|^2)=g|\psi|^2$ with $g=2$ and the potential $V\neq 0$, which is used to mode the expansion of a Bose-Einstein condensate. The initial data and potential function (see Fig. 5) are taken to be the Gaussian pulses

$$\psi(x,y,0) = e^{-0.1(x-x_0)^2-0.1(y-y_0)^2} \text{ and } V(x,y) = e^{-0.5(x-x_0)^2-0.5(y-y_0)^2} \tag{46}$$

with $x_0=y_0=15$. It is a nonlinear wave with repulsive interaction. In the calculation, we take $L=30$, $\Delta x=\Delta y=0.1$, and $\Delta t=0.01$. Figure 6 represents the contours of the numerical solution at different snapshots with $\xi_0=\eta_0=2.0$. One can see that there are no clear reflections near the boundaries and corners.

VI. CONCLUSION

We have shown that the unified approach can obtain the local absorbing boundary conditions for the two-dimensional nonlinear Schrödinger equations. The obtained local absorbing boundary conditions on the rectangle are proved to be well posed and accurate by a normal mode analysis and numerical experiments. This approach provides considerable insight into the splitting method. We expect that this unified approach can form a basis for designing the efficient absorbing boundary conditions of a class of nonlinear problems.

ACKNOWLEDGMENTS

The authors are grateful to Professor Houde Han for the fruitful discussion on constructing the LABCs and thank Professor H. Brunner for his reading. This research was supported in part by RGC of Hong Kong and FRG of Hong Kong Baptist University. We thank the two referees for their careful reading of the paper and for suggestions that led to an improved version of the paper.

[1] B. Engquist and A. Majda, Math. Comput. **31**, 629 (1977).
[2] R. L. Higdon, Math. Comput. **47**, 437 (1986).
[3] H. Han and X. Wu, J. Comput. Math. **3**, 179 (1985).
[4] D. Yu, J. Comput. Math. **3**, 219 (1985).
[5] L. Halpern and J. Rauch, Numer. Math. **71**, 185 (1995).
[6] T. Hagstrom, Acta Numerica **8**, 47 (1999).
[7] X. Antoine, A. Arnold, C. Besse, M. Ehrhardt, and A. Schädle, Commun. Comput. Phys. **4**, 729 (2008).
[8] D. Givoli, *Numerical Methods for Problems in Infinite Domains* (Elsevier, Amsterdam, 1992).
[9] S. V. Tsynkov, Appl. Numer. Math. **27**, 465 (1998).
[10] J. P. Bérenger, J. Comput. Phys. **114**, 185 (1994).
[11] G. P. Agrawal, *Nonlinear Fiber Optics*, 3rd ed. (Academic Press, San Diego, 2001).
[12] L. P. Pitaevskii and S. Stringari, *Bose-Einstein Condensation* (Oxford University Press, Oxford, 2003).
[13] C. Sulem and P. L. Sulem, *The Nonlinear Schrödinger Equation: Self-Focusing and Wave Collapse* (Springer, New York, 1999).
[14] M. M. Cerimele, M. L. Chiofalo, F. Pistella, S. Succi, and M. P. Tosi, Phys. Rev. E **62**, 1382 (2000).
[15] S. K. Adhikari, Phys. Rev. E **62**, 2937 (2000).
[16] W. Bao, D. Jaksch, and P. A. Markowich, J. Comput. Phys. **187**, 318 (2003).
[17] Y. B. Gaididei, J. Schjodt-Eriksen, and P. L. Christiansen, Phys. Rev. E **60**, 4877 (1999).
[18] H. Han and Z. Huang, Commun. Math. Sci. **2**, 79 (2004).
[19] V. A. Baskakov and A. V. Popov, Wave Motion **14**, 123 (1991).
[20] T. Fevens and H. Jiang, SIAM J. Sci. Comput. (USA) **21**, 255 (1999).
[21] J.-P. Kuska, Phys. Rev. B **46**, 5000 (1992).
[22] I. Alonso Mallo and N. Reguera, SIAM J. Numer. Anal. **40**, 134 (2002).
[23] T. Shibata, Phys. Rev. B **43**, 6760 (1991).
[24] T. Hagstrom and H. B. Keller, Math. Comput. **48**, 449 (1987).
[25] H. Han, X. Wu, and Z. Xu, J. Comput. Math. **24**, 295 (2006).
[26] X. Wu and J. Zhang, Comput. Math. Appl. **56**, 242 (2008).
[27] Z. Xu, H. Han, and X. Wu, Commun. Comput. Phys. **1**, 479 (2006).
[28] G. Strang, SIAM J. Numer. Anal. **5**, 506 (1968).
[29] W. Bao, S. Jin, and P. Markowich, SIAM J. Sci. Comput. **25**, 27 (2003).
[30] D. Lanser and J. Verwer, J. Comput. Appl. Math. **111**, 201 (1999).
[31] H. Han and Z. Zhang, J. Comput. Phys. **227**, 8992 (2008).
[32] J. Szeftel, SIAM J. Numer. Anal. **42**, 1527 (2004).
[33] Z. Xu and H. Han, Phys. Rev. E **74**, 037704 (2006).
[34] C. Zheng, J. Comput. Phys. **215**, 552 (2006).
[35] X. Antoine, C. Besse, and S. Descombes, SIAM J. Numer. Anal. **43**, 2272 (2006).
[36] J. Szeftel, Numer. Math. **104**, 103 (2006).
[37] C. Farrell and U. Leonhardt, J. Opt. B: Quantum Semiclassical Opt. **7**, 1 (2005).
[38] C. Zheng, J. Comput. Phys. **227**, 537 (2007).
[39] A. Soffer and C. Stucchio, J. Comput. Phys. **225**, 1218 (2007).
[40] P. L. Sulem and C. Sulem, Commun. Pure Appl. Math. **37**, 755 (1984).
[41] J. Zhang, Z. Xu, and X. Wu, Phys. Rev. E **78**, 026709 (2008).
[42] L. A. Khan and P. L. F. Liu, Comput. Methods Appl. Mech. Eng. **152**, 337 (1998).
[43] Z. Xu, H. Han, and X. Wu, J. Comput. Phys. **225**, 1577 (2007).
[44] H. O. Kreiss and J. Lorenz, *Initial-Boundary Value Problems and the Navier-Stokes Equations* (Academy Press, Boston, 1989).
[45] Q. Chang, E. Jia, and W. Sun, J. Comput. Phys. **148**, 397 (1999).